NeuroImage: Clinical 28 (2020) 102482

Contents lists available at ScienceDirect

NeuroImage: Clinical

journal homepage: www.elsevier.com/locate/ynicl

Locus coeruleus connectivity alterations in late-life major depressive disorder during a visual oddball task

Inés del Cerro [a,b,c], Ignacio Martínez-Zalacaín [a,b], Andrés Guinea-Izquierdo [a,b], Jordi Gascón-Bayarri [d], Vanesa Viñas-Diez [d], Mikel Urretavizcaya [a,b,c], Pablo Naval-Baudin [e], Carlos Aguilera [e], Ramón Reñé-Ramírez [d], Isidre Ferrer [f,g,h], José M. Menchón [a,b,c], Virginia Soria [a,b,c,*], Carles Soriano-Mas [a,c,i,*]

[a] Bellvitge Biomedical Research Institute-IDIBELL, Department of Psychiatry, Bellvitge University Hospital, Barcelona, Spain
[b] Department of Clinical Sciences, Bellvitge Campus, University of Barcelona, Barcelona, Spain
[c] Network Center for Biomedical Research on Mental Health (CIBERSAM), Carlos III Health Institute (ISCIII), Barcelona, Spain
[d] Dementia Diagnostic and Treatment Unit, Department of Neurology, Bellvitge University Hospital, Barcelona, Spain
[e] Imaging Diagnostic Institute (IDI), Neuroradiology Unit, Bellvitge University Hospital, Barcelona, Spain
[f] Department of Pathology and Experimental Therapeutics, Institute of Neurosciences, University of Barcelona, Barcelona, Spain
[g] Bellvitge Biomedical Research Institute-IDIBELL, Department of Pathologic Anatomy, Bellvitge University Hospital, Barcelona, Spain
[h] Network Center for Biomedical Research on Neurodegenerative Diseases (CIBERNED), Barcelona, Spain
[i] Department of Psychobiology and Methodology in Health Sciences, Universitat Autònoma de Barcelona, Barcelona, Spain

ARTICLE INFO

Keywords:
Late-life major depressive disorder
Mild cognitive impairment
Locus coeruleus
Anterior cingulate cortex
Functional magnetic resonance imaging
Visual oddball task

ABSTRACT

The Locus Coeruleus (LC) is the major source of noradrenergic neurotransmission. Structural alterations in the LC have been observed in neurodegenerative disorders and at-risk individuals, although functional connectivity studies between the LC and other brain areas have not been yet performed in these populations. Patients with late-life major depressive disorder (MDD) are indeed at increased risk for neurodegenerative disorders, and here we investigated LC connectivity in late-life MDD in comparison to individuals with amnestic type mild cognitive impairment (aMCI) and healthy controls (HCs). We assessed 20 patients with late-life MDD, 16 patients with aMCI, and 26 HCs, who underwent a functional magnetic resonance scan while performing a visual oddball task. We assessed task-related modulations of LC connectivity (i.e., Psychophysiological Interactions, PPI) with other brain areas. A T1-weighted fast spin-echo sequence for LC localization was also obtained. Patients with late-life MDD showed lower global connectivity during target detection in a cluster encompassing the right caudal LC. Specifically, we observed lower LC connectivity with the left anterior cingulate cortex (ACC), the right fusiform gyrus, and different cerebellar clusters. Moreover, alterations in LC-ACC connectivity correlated negatively with depression severity (i.e., Geriatric Depression Scale and number of recurrences). Reduced connectivity of the LC during oddball performance seems to specifically characterize patients with late-life MDD, but not other populations of aged individuals with cognitive alterations. Such alteration is associated with different measures of disease severity, such as the current presence of symptoms and the burden of disease (number of recurrences).

1. Introduction

The locus coeruleus (LC), the major noradrenergic (NA) source in the central nervous system, has been suggested to be one of the initial sites of appearance of pathologically altered tau aggregates in preclinical stages of Alzheimer's disease (AD) (Braak et al., 2011; Zarow et al., 2003; Braak and Del Tredici, 2015). Neuropathological studies have revealed that pretangle tau lesions may be observed in the LC of healthy subjects before 30 years of age (Braak and Del Tredici, 2011), and tau alterations in the LC of asymptomatic individuals have been related to alterations in different metabolic pathways of LC neurons and increased pro-inflammatory gene expression and microglia response, which are

* Corresponding authors at: Department of Psychiatry, Bellvitge University Hospital, Bellvitge Biomedical Research Institute-IDIBELL, Feixa Llarga s/n, 08907, L'Hospitalet de Llobregat, Barcelona, Spain.
E-mail addresses: vsoria@bellvitgehospital.cat (V. Soria), csoriano@idibell.cat (C. Soriano-Mas).

https://doi.org/10.1016/j.nicl.2020.102482
Received 24 April 2020; Received in revised form 25 September 2020; Accepted 19 October 2020
Available online 27 October 2020

accompanied by compensatory increases in α2A adrenergic receptor protein levels in regions receiving noradrenergic input from the LC, such as the amygdala or the hippocampus (Andrés-Benito et al., 2017).

Individuals with mild cognitive impairment (MCI), with an estimated AD-conversion rate around 10–15% per year (Petersen, 2004), accumulate tau pathological changes in the LC to a larger extent than cognitively preserved individuals (Grudzien et al., 2007). Such accumulation, however, is smaller than in AD, suggesting that LC degeneration increases throughout the MCI-AD continuum (Grudzien et al., 2007). Moreover, individuals with amnestic MCI (aMCI), with AD conversion odds greater than the non-amnestic subtype (Busse et al., 2006), also present alterations in pupillary response (Granholm et al., 2017), which has been shown to be associated to altered task-induced phasic activity of LC neurons (Elman et al., 2017), although pupil dilation may also depend on other neurotransmitter systems, such as serotonin (Weinberg-Wolf et al., 2018).

Subjects with late-life major depressive disorder (MDD) have a twofold increased risk of progression to AD (Byers and Yaffe, 2011; Green et al., 2003), and also show alterations in the LC, such as a decreased neuronal count (Baumann et al., 1999). More importantly, MDD patients present a decreased neuron density in LC projection areas (e.g., hippocampus or prefrontal cortex) (Tsopelas et al., 2011), which has led to suggest that decreased NA input may be related to neural degeneration in different brain regions (Gannon and Wang, 2019). Nevertheless, to our knowledge, no previous studies have evaluated potential abnormalities in the connectivity between the LC and the multiple areas receiving NA input in late-life MDD. This could be achieved by non-invasive means with functional magnetic resonance imaging (fMRI) estimations of functional connectivity between the LC and the rest of the brain.

In physiological conditions, phasic discharge in LC neurons occurs in front of salient events (Aston-Jones and Cohen, 2005), and NA activity has been linked to fast orienting and flexible behavior by optimizing signal-to-noise ratio in regions receiving LC input (Devilbiss, 2004). In experimental settings, such phasic activity of the LC has been traditionally assessed by means of oddball paradigms (Rajkowski et al., 1994) evaluating the capacity to rapidly detect unpredictable, infrequent and salient stimuli (i.e., oddball stimuli) (Aston-Jones et al., 1994). Despite the limited temporal resolution of BOLD fMRI, putative alterations in functional connectivity between the LC and the rest of brain areas should therefore be better captured during event-related tasks than during resting-state or blocks of continuous activation.

Here, we aim to evaluate whole-brain functional connectivity of the LC during a visual oddball paradigm in patients with late-life MDD, who were compared to patients with aMCI and healthy controls (HCs). We also aimed at correlating neuroimaging measurements with clinical and neuropsychological data. Importantly, although the oddball task has been strongly associated with LC and NA activity, to evaluate the specificity of our potential findings, we first performed a global connectivity degree analysis (i.e., voxel-to-voxel, or V2V) to identify voxels showing functional connectivity alterations during oddball detection within a pons area encompassing different nuclei that could be also involved in oddball detection. Such an approach also allowed for detecting significant differences in distinct LC subregions. Moreover, to ascertain that our findings were indeed located in the LC, our functional findings were contrasted against a specific structural sequence allowing visualization of the LC. Finally, we performed a seed-based analysis with the results from the V2V analysis to characterize LC connectivity. We hypothesized that individuals with late-life MDD and aMCI will show impairment in the oddball task in combination with a disrupted connectivity from the LC to other brain areas during oddball detection, and this will likely relate to measures of task performance and disorder severity. We also anticipate that such alterations will discriminate between the clinical groups.

2. Methods

2.1. Participants

The final sample of the study included 20 patients with late-life MDD (13 women), 16 aMCI (10 women) and 26 HCs (16 women) (see Table S1 for a description of the number of participants initially recruited and the reasons for their exclusion). Late-life MDD patients were consecutively recruited from the Department of Psychiatry at Bellvitge University Hospital (Barcelona, Spain), and diagnosed following DSM-IV-TR criteria for MDD. In all cases, major depression was their primary diagnosis, and the first depressive episode appeared after 40 years of age. Individuals with aMCI were consecutively recruited from the Department of Neurology of the same hospital. They were diagnosed following Petersen criteria[6], with Clinical Dementia Rating (CDR) scores of 0.5 (Hughes et al., 1982), and were characterized as amnestic MCI using the delayed recall test (5 points or less) of the Wechsler Memory Scale III (Wechsler, 1997). Importantly, aMCI subjects did not present MDD comorbidity. It is important to note that our definition of aMCI is based on a syndromal categorical cognitive staging approach, and not in the use of biomarkers (Jack et al., 2018). Healthy controls were recruited from the same geographical area through advertisements and underwent a medical anamnesis to rule out the possibility of current or lifetime psychiatric or neurologic disorder, as well as the use of psychotropic medication.

All participants underwent a comprehensive neuropsychological testing, including the Mini Mental State Examination (MMSE) (Folstein et al., 1975) and different tests covering the domains of attention, verbal learning and memory, executive functioning, language, visual gnosias and motor praxis (Table S2). Since groups differed in premorbid intelligence (i.e., Vocabulary score, $F_{(2,59)} = 24.99$, $p < 0.0001$), this variable was used as confounding covariate in across-group comparisons of neurocognitive variables. The Spanish brief version of the Geriatric Depression Scale (GDS) (Martínez de la Iglesia et al., 2002) and the Hamilton Depression Rating Scale (Hamilton, 1960) were administered to assess depression severity, but not for diagnostic purposes, and the Functional Assessment Staging scale (FAST) (Sclan and Reisberg, 1992) was used as a measure of functionality.

Exclusion criteria included < 60 or > 75 years, current or past history of other psychiatric or neurological disorders, acute and severe depressive symptoms hampering neurocognitive assessment, a Hachinski Ischemia Score > 3, CDR scores > 0.5, mental disability, any severe medical condition, current or past substance abuse (excluding nicotine), sensorial impairment preventing undertaking any of the assessments, presence of contraindications to magnetic resonance imaging (MRI), or gross abnormalities in the MRI scan. Written informed consent was obtained from all participants after a complete description of the study, which was performed in accordance with the Declaration of Helsinki and approved by the ethical committee in clinical research of Bellvitge University Hospital.

2.2. Visual oddball task

All participants undertook a visual oddball task during the acquisition of an fMRI sequence. They were instructed to lie still without moving, focusing their attention on a centrally presented visual stimuli consisting of a purple cross (0.65° of the visual angle) and standard and target/oddball stimuli (purple circles with diameters subtending 3.2° and 1.6° of the visual angle, respectively). All stimuli were presented against a dark-grey background matched for luminance. A total of 200 standard stimuli and 50 targets were presented for 100 ms each, with an interstimulus interval pseudorandomly varying between 2.5 and 3.5 s. Target stimuli (20% of the trials) were pseudorandomly distributed throughout the task ensuring a minimum inter-target interval of 10 s. Finally, seven 14 s cross blocks were interspersed throughout the task to minimize fatigue. Task was presented using E-Prime software

(Psychology Software Tools Inc., Pittsburgh, PA) and a 32 LCD Bold Screen for fMRI (Cambridge Research Systems Ltd) placed at the rear of the bore, which was visible though a mirror mounted at the MRI head coil. Subjects indicated the detection of the oddball stimuli with a right-handed index-press using an MRI-compatible three-button fiber optic response box (Lumina 3G Controller, Cedrus Corporation). Task duration was 14 min 42 s.

2.3. Image acquisition

Imaging data were acquired using a 3 T Ingenia scan (Philips Healthcare, Best, The Netherlands) equipped with a 32-channel head coil at Imaging Diagnostic Institute (IDI, Duran i Reynals Hospital, Barcelona, Spain). The functional sequence consisted of 435 echo-planar image volumes (excluding the four initial dummy volumes) comprising 40 interleaved slices acquired in the oblique axial direction perpendicular to the floor of the fourth ventricle (repetition time = 2000 ms; echo time = 25 ms; flip angle = 90°; 3 mm isotropic voxels; field of view = 24 cm, 80x80 pixel matrix).

For anatomical reference and imaging preprocessing purposes, we also acquired for each participant a whole-brain T1-weighted anatomical three-dimensional inversion-recovery prepared spoiled gradient echo sequence (233 axial slices; repetition time = 10.46 ms; echo time = 4.79 ms; flip angle = 8°; 0.75 mm isotropic voxels; field of view = 24 cm; pixel matrix = 320 × 318; total duration = 5 min, 04 s).

Moreover, a T1-weighted fast spin-echo sequence was also acquired for LC localization. This sequence lasted 15 min 02 s and consisted of 15 slices covering the brainstem area to the level of the caudal pons with the following parameters: repetition time = 600 ms; echo time = 14 ms; flip angle = 90°; 2.5 mm slice thickness; 0 mm gap; matrix size 404x250; FOV 170x170 mm^2; acquisition voxel size 0.42x0.68x2.5 mm^3; reconstructed voxel size 0.39x0.39x2.5 mm^3). The sections were acquired in the oblique axial direction perpendicular to the floor of the fourth ventricle covering from the posterior commissure to the inferior border of the pons. See supplementary material for details on LC localization, and Figs. S1 and S2. Throughout the acquisition protocol, we used foam pads and made sure that patients' head was comfortably placed within the head coil to avoid excessive movement.

2.4. Imaging data preprocessing and denoising

First, functional time series were initially despiked using the BrainWavelet toolbox v2.0 (Patel et al., 2014). Next, using MATLAB version 9.3 (R2017b) (The MathWorks Inc, Natick, Massachusetts) and the MATLAB-based CONN-fMRI Functional Connectivity toolbox version 17.f (Whitfield-Gabrieli and Nieto-Castanon, 2012), implemented in SPM12 (Wellcome Department of Imaging Neuroscience, London, UK; www.fil.ion.ucl.ac.uk/spm), functional images were aligned to the first volume of the time series using a six-parameter rigid body spatial transformation and a least-squares minimization in combination with an unwarping algorithm aimed at correcting motion and motion-related distortions. Slice-timing correction was then applied. The ART-based automatic volume outlier detection (https://www.nitrc.org/projects/artifact_detect/) was also run for later scrubbing. Likewise, both functional and structural images were subjected to simultaneous grey, white matter and cerebrospinal fluid segmentation, and a bias correction was performed to remove smoothly varying intensity differences across images. Such image segments were subsequently spatially normalized through non-linear transformations to the Montreal Neurological Institute (MNI) stereotactic space, and images were resliced to a 2-mm isotropic resolution. Finally, images were smoothed with an 8-mm full-width at half-maximum (FWHM) isotropic Gaussian kernel.

After preprocessing, data were denoised from residual movement and physiological noise. Denoising steps included a temporal despiking, regressing out confounding factors (i.e., effect of BOLD signal small ramping effects at the beginning of each scan session and the six rigid body realignment parameters, as well as their first order derivatives), controlling for total grey matter (GM) signal, linear detrending, the ART scrubbing protocol, and band-pass filtering (0.008–0.09 Hz). The ART scrubbing protocol regressed out the effect of outlier volumes which signal intensity deviated >5 standard deviations from whole series mean signal intensity or showed evidence of displacement superior to 0.9 mm in relation to the preceding volume. Finally, physiological noise was removed with the anatomical component-based noise correction method (aCompCor) (Behzadi et al., 2007). Importantly, after implementing these different steps, none of the subjects was removed from the analysis because, according to current guidelines (Satterthwaite et al., 2013; Van Dijk et al., 2010), all individual functional series included at least a 95% of original volumes after scrubbing. Moreover, the number of outlier volumes did not differ across the study groups.

2.5. Functional MRI data analysis: task-related connectivity

Changes in LC connectivity over time were also assessed using the CONN toolbox v17.f (Whitfield-Gabrieli and Nieto-Castanon, 2012). Specifically, analyses were divided in two parts: voxel-to-voxel and generalized psychophysiological interactions analysis.

2.5.1. Voxel-to-voxel analysis (V2V)

We performed an Intrinsic Connectivity Contrast (ICC) analysis (Martuzzi et al., 2011), which provides an estimation of the number of significant (positive or negative) V2V connections and therefore allowed characterizing global connectivity strength between each voxel and the rest of the brain during oddball detection in relation to standard stimuli. In first-level (within-subject) analyses, the matrix of V2V bivariate correlation coefficients was computed for each participant using the residual BOLD time series from all the 2-mm isotropic gray matter voxels of a whole-brain mask. The correlations of each voxel with the rest of brain voxels were then averaged and displayed in a brain map format as beta-values representing the strength of the whole-brain correlations for each voxel. Realignment parameters, scan-to-scan changes in global BOLD signal (Z-scores), framewise displacement timeseries (in mm) and outlier scans were included as nuisance parameters in this analysis. Next, in the second level (between-subject) analysis, we used the individual beta-maps from the first level analysis to estimate a one-way ANOVA model and compare the voxel-wise connectivity strengths across the three study groups. In accordance with our hypothesis, however, this second-level analysis was restricted to pons voxels to specifically assess across-group changes in global connectivity strength from these areas to the rest of the brain. For this, we used a pons parcellation from the WFU PickAtlas toolbox (Maldjian et al., 2003) encompassing gray matter voxels from the pontine tegmentum, where the LC and other nuclei are located, and the basilar pontine nuclei in the ventral-caudal pons (see Fig. S3).

2.5.2. Generalized psychophysiological interactions analysis (gPPI)

We performed a gPPI analysis to study the specific LC task-related connectivity and identify the brain regions showing more significant changes in connectivity with the LC between target and standard conditions (contrast oddball > standard stimuli). Specifically, we assessed the influence of the task ('psychological factor') on the strength of time-course correlations between signal from the peak cluster resulting from the above ICC analysis and signal from all other brain voxels ('physiological factor'). The resulting contrast images were used in subsequent one-way ANOVA analyses (second-level) to assess across-group differences in task-induced changes in connectivity between the LC and the rest of the brain.

All analyses were controlled for age and sex. Moreover, to set a multiple comparison corrected significance threshold, a voxel-wise non parametric permutation testing with 5000 permutations (Nichols and Holmes, 2001) using the Threshold-Free Cluster Enhancement (TFCE) method (Smith and Nichols, 2009, SPM-TFCE toolbox v138: http://dbm.

neuro.uni-jena.de/tfce/) was applied. Statistical significance was set at $p < 0.05$, Family-Wise Error (FWE) corrected across all voxels of interest. Finally, to confirm our findings were indeed involving the LC, results from V2V analyses were overlapped onto the MNI-normalized LC map of our sample (see Supplementary material for details).

2.5.3. Correlations between imaging and clinical and neuropsychological variables

To explore for the potential association of imaging with clinical and neuropsychological variables, we extracted the first eigenvariate (the factor accounting for the highest percentage of variance of voxel values within a cluster) of significant clusters in above analyses and conducted a series of correlations using SPSS v.25 (SPSS Inc., Chicago, IL). Partial correlations (controlling for age), were performed between imaging results and measures of oddball performance, severity scores (i.e., GDS and MMSE), and other clinical variables such as age at disorder's onset, number of MDD recurrences, and delayed memory scores, and non-parametric statistics were used in post-hoc analyses involving a limited number of subjects (see Results section below). Transformations were applied when the distribution of variables deviated from normality (i.e., skewness). Given the exploratory nature of these analyses, significance threshold was set at $p < 0.05$.

3. Results

3.1. Sociodemographic, clinical and neuropsychological characteristics

Sociodemographic, clinical and neuropsychological characteristics of all participants are described in Table 1 and Table S3. Overall, we observed significant across-group differences in clinical and different neuropsychological domains and oddball task performance. Scheffé's post hoc tests showed that, overall, MDD and aMCI groups performed worse than HCs. Specifically, MDD presented higher GDS scores and lower MMSE compared to HCs, and higher HDRS scores in comparison to the other two groups. aMCI individuals showed lower scores in the MMSE, the FAST and executive functioning. Memory impairments were present in aMCI in comparison to both MDD and HCs. As for the oddball task, both clinical groups made more omission errors than HCs, and aMCI subjects made more commission errors than MDD and HCs groups.

Table 1
Sociodemographic and clinical characteristics of the study participants.

	MDD (n = 20)	aMCI (n = 16)	HCs (n = 26)			
	Mean (SD)	Mean (SD)	Mean (SD)	F	*df*	*p* Value
Age, years	67.05 (4.31)	71.13 (2.83)	67.42 (4.33)	5.606		0.006*
Number of depressive recurrences	3.35 (1.69)					
GDS	5.27 (4.88)	2.79 (2.42)	0.85 (1.14)	10.717	60	0.001*,‡
HDRS	10.27 (6.70)	3.93 (3.13)	0.90 (1.33)	23.377	61	0.001*,†,‡
FAST	18.73 (10.07)	25.07 (15.56)	13.70 (10.97)	3.966	61	0.024*,§
MMSE	26.67 (2.23)	25.86 (2.41)	29.15 (1.14)	14.784	60	0.001*,‡,§
Oddball task						
Reaction time	452.61 (86.21)	453.77 (105.36)	429.71 (44.21)	0.504	60	0.607
Commission errors	5.47 (4.55)	17.79 (23.75)	2.60 (1.79)	7.239	58	0.002*,†,§
Omission errors	6.13 (6.26)	6.00 (5.34)	2.80 (3.43)	3.210	60	0.048*
Vocabulary WAIS-III	28.10 (7.78)	31.44 (8.72)	45.08 (9.18)	24.986	59	0.001*,‡,§

Abbreviations: aMCI = amnestic type mild cognitive impairment individuals; FAST = Functional Assessment Staging; GDS = Geriatric Depression Scale; HCs = healthy controls; HDRS = Hamilton Depression Rating Scale; MDD = late-life major depression disorder; MMSE = Mini-mental State Examination; SD = standard deviation.
Post-hoc tests of pair-wise differences.
* $p < 0.05$ after FDR correction.
‡ MDD – HCs.
† MDD – aMCI.
§ aMCI – HCs.

3.2. Functional connectivity results

3.2.1. Global connectivity

In comparison to aMCI and HC groups, MDD patients showed lower global connectivity strength during oddball trials in relation to standard trials from a cluster located in the right caudal LC (peak voxel: x = 6, y = -38, z = -36; TFCE = 54.11; kE = 10; pFWE = 0.035) to other gray matter voxels throughout the brain (Fig. 1). To confirm the location of this finding, we overlapped the functional cluster onto the LC distribution map obtained from our sample, what confirmed that the cluster was located at the most caudal portion of the LC (Fig. 1A). Importantly, to further confirm the specificity of our findings and the effects of signal from surrounding structures, we estimated across-group differences from 5 additional seeds in the pontine tegmentum and 2 additional seeds in the fourth ventricle. All analyses reported null findings (see Figs. S4 and S5). When exploring results at a more lenient threshold ($p < 0.01$, uncorrected), a similar cluster appeared in the left hemisphere, with the peak coordinate at x = -4, y = -38, z = -30, although this result did not survive TFCE correction.

3.2.2. gPPI results

In the oddball > standard contrast, MDD patients showed, in comparison to HCs, lower positive connectivity between the right caudal LC cluster from the above analysis and the left anterior cingulate cortex (ACC), the right fusiform gyrus (FG) and the right cerebellum. When compared to aMCI, we observed lower positive connectivity between the right caudal LC and the posterior cerebellum in MDD patients during oddball stimuli detection as compared to standard stimuli. No differences were observed between aMCI and HCs (see Table 2 and Fig. 2A, C-E).

Finally, in the MDD group, connectivity between the LC and the ACC correlated inversely with GDS score ($r = -0.471$, $p = 0.036$). As can be seen in Fig. 2B, this correlation was indeed reflecting that we had two groups of subjects, those in active depression episode (n = 7) and those asymptomatic (n = 13). These two groups differed not only in their GDS scores (below and above the 4–5 points used as cut-off), but also in their LC-ACC PPI estimates (Mann-Whitney's U = 17; Z = −2.26; p = 0.024). We also observed a significant negative correlation with the number of recurrences (Ln transformed; $r = -0.507$, $p = 0.022$) (Fig. 2B). These analyses were controlled for age. Controlling for psychotropic medication intake (15 patients were taking dual noradrenaline-serotonin antidepressants, while 5 subjects were taking SSRIs) did not modify our findings. We detected no further correlations between gPPI results and the rest of clinical and performance variables, including the number of errors.

4. Discussion

In this study, we used an attentional oddball paradigm to assess subjects with late-life MDD in comparison to individuals with aMCI and HCs. Significant alterations in LC connectivity were specifically observed in the MDD group, and, remarkably, such alterations were associated with clinical severity. Therefore, our results suggest that disrupted connectivity of the LC characterizes individuals with late-life MDD, scaling with disease severity. Contrary to our expectations, however, the aMCI group did not show evidence of LC connectivity alteration, although this group showed an impaired task performance.

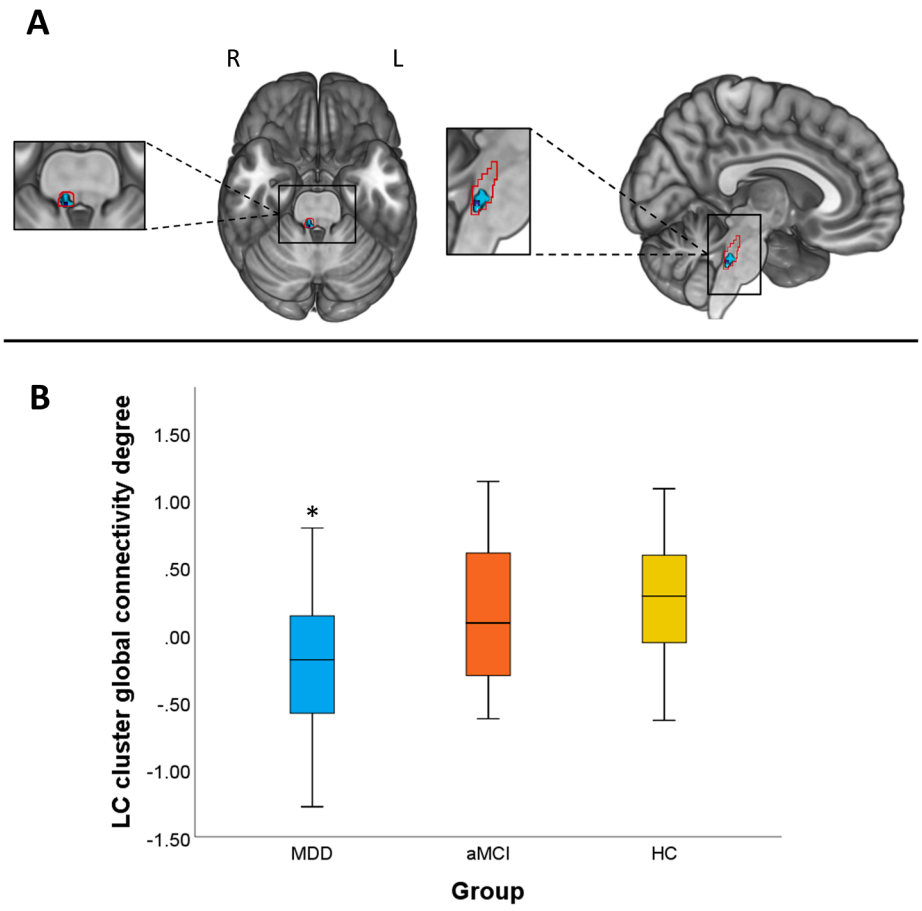

Fig. 1. Global connectivity results. Patients with late-life MDD showed lower global connectivity degree in the right caudal LC in comparison to aMCI and HC groups. (A) Basal and sagittal view of the LC cluster (in light blue) and peak coordinate (dark blue) ($p_{FWE} < 0.05$, TFCE corrected). The cluster is overlaid onto the LC study-specific mask (red contour, see Supplementary material for details). This mask was down-sampled to the resolution of the functional time-series. As can be observed, our cluster was located in the most caudal part of the LC. (B) Box-plot depicting global connectivity degree of the right caudal LC cluster for the three study groups. Values in the Y axis are normalized to fit a Gaussian distribution with zero mean and unitary variance, and, therefore, negative values should not be interpreted as negative connectivity. L = Left, R = Right. $^{*}p_{FWE} < 0.05$. (For interpretation of the references to colour in this figure legend, the reader is referred to the web version of this article.)

Table 2
Between-group differences in LC connectivity during the oddball task.

Contrast	Region	MNI Coordinates (x, y, z)	kE	*p* value[†]	TFCE value
MDD < HCs	Left anterior cingulate cortex	−2, 32, 20	76	0.028	413.75
	Right fusiform gyrus	40, −48, −24	1100	0.002	602.65
	Vermis lobule VIII	6, −58, −28	115	0.033	403.21
	Right Cerebellum lobe III	10, −38, −18	14	0.036	397.86
	Right Cerebellum lobe VIII	34, −50, −56	162	0.013	466.62
	Right Cerebellum lobe IX	8, −56, −42	64	0.022	431.80
MDD < aMCI	Right Cerebellum lobe III (extending to Left lobe III)	8, −36, −16	372	0.001	662.75

Abbreviations: aMCI = amnestic type mild cognitive impairment individuals; HCs = healthy controls; kE = cluster extent; MDD = late-life major depressive disorder patients; MNI = Montreal Neurological Institute, TFCE = Threshold-Free Cluster Enhancement.

[†] All p-values were FWE-corrected, $p < 0.05$.

Specifically, although the clinical groups, when tested against controls, displayed more omission errors, only aMCI individuals showed a higher number of commission errors during oddball performance, which concurs with previous reports (Tsolaki et al., 2017).

Individuals with late-life MDD displayed lower LC connectivity with other brain regions. The role of the LC in depression has been evidenced in previous research, ranging from a loss of NA neurons (Chan-Palay and Asan, 1989), to intra and extra neuronal signaling pathway alterations (Bernard et al., 2011). Moreover, chemical damage to the LC with selective neurotoxins has been associated to depressive-like behaviors (Szot et al., 2016), such as reduced exploratory activity (van den Buuse et al., 2001), fewer social interactions (Cornwell-Jones et al., 1992), or increased immobility in the forced swim test (Harro et al., 1999). Interestingly, our findings were lateralized to the right LC, although, when lowering the significance threshold, we also observed similar alterations in the left LC. Why in our patients with MDD this alleged pathological processes seems to start in the right hemisphere remains an open question.

Our findings were also located in the most caudal portion of the LC. Although neurons from this location have been reported to be preferentially connecting to the spinal cord (Nakazato, 1987), we observed functional connectivity alterations from there to brain regions such as the ACC and the FG, as well as to the cerebellum. Previous research has shown that, notwithstanding the fact that the LC is not entirely homogeneous, neurons projecting to cortical targets may be scattered throughout the LC (Schwarz and Luo, 2015). Moreover, it has been observed that LC neurons receive input from at least 9–15 different brain regions, which suggests that neural activity in the LC is largely integrative (Schwarz et al., 2015), and is in agreement with our findings showing that the same cluster displays connectivity alterations with cortical and cerebellar regions. The location of our findings in the caudal part of the LC may therefore be the result of the interaction of multiple factors, including the specific clinical groups assessed and the task selected, as well as the existence of a rostro-caudal gradient of neural loss and dysfunction related to age and neurodegeneration staging (Theofilas et al., 2017). In this sense, patients with aMCI have been reported to show connectivity alterations from the LC during resting-state in relation to episodic memory (Jacobs et al., 2015), and the possibility exists that they will show impaired connectivity during oddball

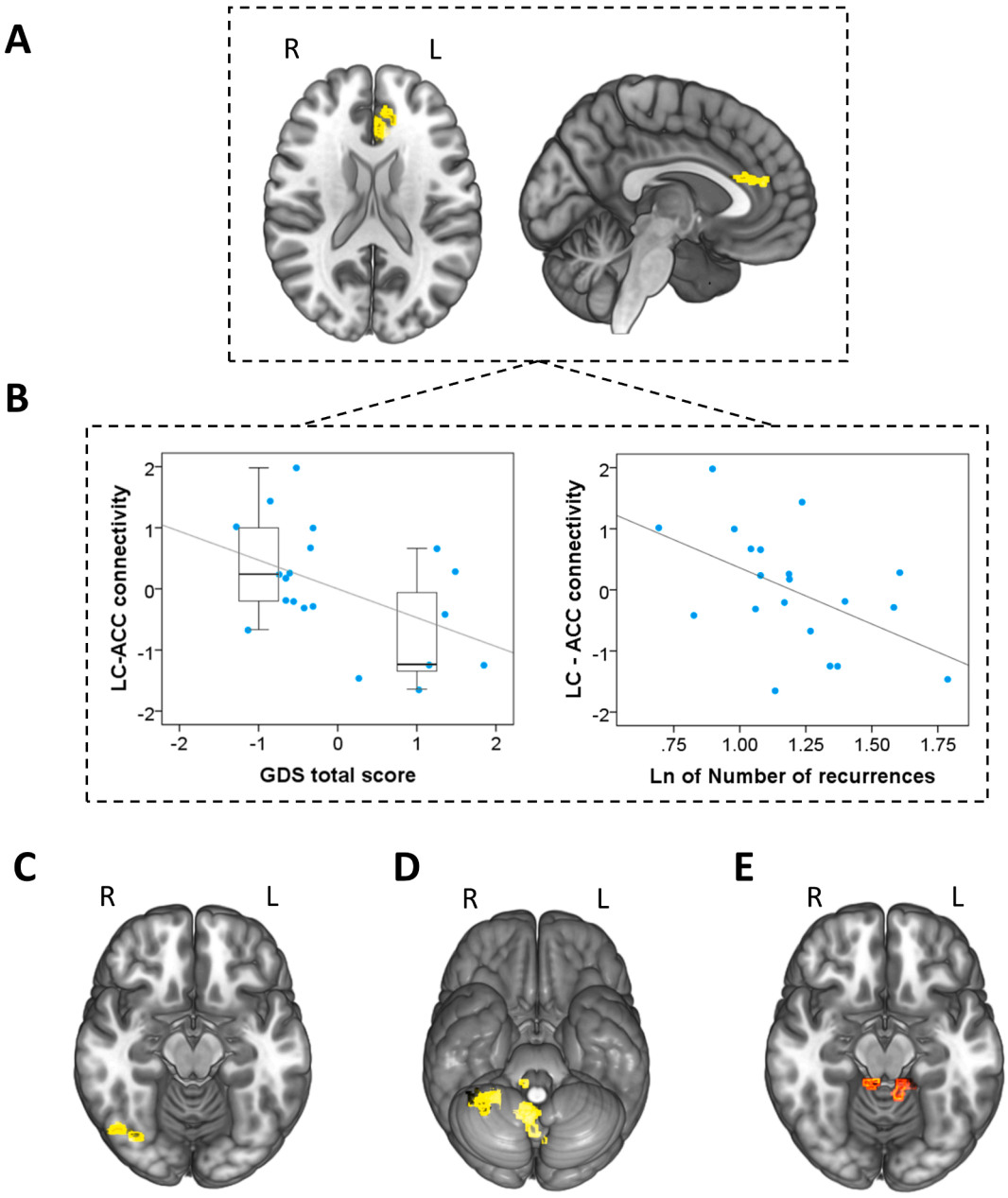

Fig. 2. gPPI results. (A) In comparison to HCs, the MDD group showed lower functional connectivity between the right LC and the left anterior cingulate cortex. (B) Scatter plots depicting the negative correlations between connectivity of the right LC with the left ACC and total Geriatric Depression Score (GDS) (left), and the number of depressive recurrences (Ln transformed, right). In the left plot, the qualitative distinction between asymptomatic patients and those in active depression episode is depicted with boxplots. Values in plots are age-adjusted. (C) The functional connectivity between LC and the right fusiform gyrus, (D) the lobule VIII of the vermis, and the right cerebellar lobules III, VIII and IX was also lower in MDD patients in comparison to HCs. (E) In comparison to the aMCI group, patients with MDD showed lower connectivity between the right LC and the bilateral cerebellar lobule III. L = Left, R = Right.

performance from this caudal location at more advanced disease stages, in relation to advanced age and neurodegenerative staging. Nevertheless, some of the previous studies showing functional LC alterations in aMCI (Granholm et al., 2017; Elman et al., 2017) did not exclude patients with comorbid depression, while our aMCI sample was free from this confounding effect. This may also partially account for the lack of LC connectivity findings reported here in individuals with aMCI. In any case, since we did not make use of any imaging or cerebrospinal fluid biomarker, we cannot confirm that these subjects belong to the AD continuum and will eventually develop AD, which must be considered a study limitation.

Regarding the regions showing lower LC input, the ACC has been consistently reported to show functional alterations in MDD (Bürger et al., 2017). Such reduced connectivity between the LC and the ACC presumably involves both ascending and descending projections (Aston-Jones and Cohen, 2005). As a central node of the salience network (Menon and Uddin, 2010), the ACC is involved in the detection of relevant stimuli through an adequate arousal inducing NA input (Gompf et al., 2010). At the same time, ACC efferent neural signals reach the LC to inform about performance related costs associated with task difficulty and processing conflicts (Aston-Jones and Cohen, 2005). Positive benefit-cost ratios may shift LC activity into phasic mode, which allows accurately engaging in task performance (Aston-Jones and Cohen, 2005).

Moreover, it is also important to highlight that disrupted connectivity between the LC and the ACC was associated with MDD severity

(GDS scores and number of recurrences), indicating that benefit-cost attentional processes may be increasingly impaired with both current symptom severity and disease burden. Structural ACC abnormalities have indeed been previously related to disease severity in MDD (Bijsterbosch et al., 2018; Satterthwaite et al., 2016). Notably, the correlation with GDS scores was indeed the result of a qualitative difference between asymptomatic patients and those in an active depressive episode, which suggests that LC-ACC connectivity may be a state marker in late-life MDD.

We also observed reduced connectivity in MDD between the LC and the FG, a region robustly related to both neutral (Strange et al., 2000) and emotional oddball stimuli processing (Aleman et al., 2008). During visual attentional tasks, the FG may show hyperreactivity to distracters in patients with MDD, hampering performance (Robertson et al., 2007). Interestingly, treatment with the dual action antidepressant bupropion, which increases synaptic NA levels, modulates such hyperreactivity to distracters in the latter study. This result concurs with our findings and the alleged role of NA in increasing signal-to-noise ratio (Aston-Jones and Waterhouse, 2016), which should result in enhanced focused attention.

Finally, the LC of MDD patients also showed lower functional connectivity with the cerebellum, mainly encompassing the vermis and the posterior cerebellar lobes. Anatomical connections between the LC and the cerebellum have been well established (Sara and Bouret, 2012), and NA connections between these two structures have been implicated in attentional orienting and sensorimotor processing of salient stimuli (Zhang et al., 2016), alterations of arousal state (Song et al., 2017), learning and memory processes through modulation of inhibitory neurotransmission in Purkinje neurons (Hoffer et al., 1973), and enhanced synaptic plasticity resulting from improvements in signal-to-noise ratio of evoked activity (Gould et al., 1997). The vermis and the posterior cerebellar lobes are also densely connected with high-order cognitive regions such as the prefrontal, parahippocampal or cingulate cortices, and, consequently, decreased NA input to the cerebellum may indirectly alter neural processing in such areas (Arrigo et al., 2014; Kelly and Strick, 2003). Indeed, abnormal functional connectivity between the cerebellum and fronto-parieto-temporal regions has been shown in MDD samples (Yin et al., 2015).

This is the first study comparing functional preservation of the LC in two clinical groups by means of an interregional correlation analysis during a visual oddball task. Moreover, since the LC is a tiny structure difficult to localize in fMRI time-series, our functional findings were overlaid onto a study-specific LC map, which confirmed the precise location of our findings in the most caudal part of the nucleus. In any case, some limitations should be acknowledged. Despite all participants were carefully characterized at the clinical and neuropsychological level, because of our naturalistic and consecutive recruitment strategy, the aMCI group was somewhat older that the other two groups. Nevertheless, age was controlled for in all analyses, and the main results of the study involved the MDD group, which did not differ in age from HCs. Likewise, our study would have probably benefited from the comparison with a group of younger patients with MDD, what would have also allowed to ascertain whether the reported findings characterize the MDD phenotype regardless of the age of the subjects. Moreover, our group patients with aMCI included fewer participants that the other two groups, which may have limited the power to detect significant differences. The methods employed in this study do also have some limitations. More specifically, our functional sequence was acquired with large voxels and we used a large smoothing kernel, which was needed to keep a good signal-to-noise ratio, certainly at the expenses of a greater spatial resolution. Further research with high-field MRI is warranted to overcome this issue (see, for instance, Jacobs et al. (2020)). BOLD fMRI, in addition, does not probably allow to detect fast changes in neuronal firing related to shifts from tonic to phasic activity in the LC. In this case, it might be of interest to combine fMRI with methods of higher temporal resolution. Finally, our correlation analyses between imaging and clinical data were exploratory and not corrected for multiple comparisons, and should therefore be interpreted with caution.

In conclusion, this study provides the first evidence of altered functional connectivity of the LC in patients with late-life MDD. Although previous research has identified AD-related neuropathological signs in this noradrenergic source, we have not detected any significant alteration in patients with aMCI, and, therefore, our finding seems to specifically characterize the late-life MDD phenotype. In this sense, we have also observed that connectivity alterations from the LC involved different brain areas, such as the ACC, relevantly involved in MDD pathophysiology, and such alterations were related to current clinical severity and burden of disease. Further research assessing the putative modulation of our results by noradrenergic agents, such as dual action antidepressants, will elucidate whether interventions on the noradrenergic system may be considered as the first-line treatment option for patients with late-life MDD.

Declaration of Competing Interest

The authors report no biomedical financial interests or potential conflicts of interest regarding this work. Dr. Soria served as a consultant or continuing medical education (CME) speaker for Lundbeck, Otsuka, Janssen-Cilag, Exeltis. Dr. Urretavizcaya has received compensation for lectures, advisories, or grants from Janssen-Cilagand, Lundbeck. Dr. Menchón has received grants and served as a consultant, advisor or CME speaker for Janssen-Cilag, Lundbeck, Medtronic, Otsuka. All other authors have nothing to disclose nor have any financial relationships with commercial interests.

Acknowledgments

The authors are grateful to all of the study participants and their families, and to the staff and technicians of Bellvitge University Hospital and Duran i Reynals Hospital who helped to recruit the sample for this study. We thank CERCA Programme / Generalitat de Catalunya for institutional support.

Funding

This study was supported by the Agency for Management of University and Research Grants of the Catalan Government (2017SGR1247), the Department of Health of the Generalitat de Catalunya (PERIS grant SLT002/16/249), the Carlos III Health Institute, Spain (Grant PIE14/00034 and CIBERSAM), and FEDER Funds/European Regional Development Fund (ERDF) ('A way to build Europe'). IdC is supported by CIBERSAM and previously by a Ph.D. FI Grant from AGAUR-Catalan Government (2016FI_B 00712), grant co-funded by the European Social Fund (ESF) "ESF, Investing in your future". IM-Z is supported by a P-FIS grant (FI17/00294) from the Carlos III Health Institute (Spain). AG-I was supported by a FPU 14/04822 grant. MU has been funded by the Carlos III Health Institute through the Spanish Ministry of Economy and Competitiveness. IF is supported by CIBERNED and JMM has received grants from the Spanish Ministry of Economy and Competitiveness and CIBERSAM. VS has received grants from the Institute of Health Carlos III through the Spanish Ministry of Economy and Competitiveness and CS-M is supported by a Miguel Servet contract (CPII16/00048) from the Carlos III Health Institute (Spain).

Appendix A. Supplementary data

Supplementary data to this article can be found online at https://doi.org/10.1016/j.nicl.2020.102482.

References

Aleman, A., Swart, M., 2008. Sex differences in neural activation to facial expressions denoting contempt and disgust. Baune B, editor. PLoS One 3 (2008) e3622.

Andrés-Benito, P., Fernández-Dueñas, V., Carmona, M., Escobar, L.A., Torrejón-Escribano, B., Aso, E., Ciruela, F., Ferrer, I., 2017. Locus coeruleus at asymptomatic early and middle Braak stages of neurofibrillary tangle pathology. Neuropathol. Appl. Neurobiol. 43 (5), 373–392. https://doi.org/10.1111/nan.12386.

Arrigo, A., Mormina, E., Anastasi, G.P., et al., 2014. Constrained spherical deconvolution analysis of the limbic network in human, with emphasis on a direct cerebello-limbic pathway. Front. Hum. Neurosci. 8, 987.

Aston-Jones, G., Cohen, J.D., 2005. Adaptive gain and the role of the locus coeruleus-norepinephrine system in optimal performance. J. Comp. Neurol. 493 (1), 99–110. https://doi.org/10.1002/cne.20723.

Aston-Jones, G., Cohen, J.D., 2005. An integrative theory of locus coeruleus-norepinephrine function: adaptive gain and optimal performance. Annu. Rev. Neurosci. 28 (1), 403–450. https://doi.org/10.1146/annurev.neuro.28.061604.135709.

Aston-Jones, G., Rajkowski, J., Kubiak, P., Alexinsky, T., 1994. Locus coeruleus neurons in monkey are selectively activated by attended cues in a vigilance task. J. Neurosci. 14 (7), 4467–4480. https://doi.org/10.1523/JNEUROSCI.14-07-04467.1994.

Aston-Jones, G., Waterhouse, B., 2016. Locus coeruleus: from global projection system to adaptive regulation of behavior. Brain Res. 1645, 75–78. https://doi.org/10.1016/j.brainres.2016.03.001.

Baumann, B., Danos, P., Krell, D., Diekmann, S., Wurthmann, C., Bielau, H., Bernstein, H.-G., Bogerts, B., 1999. Unipolar–bipolar dichotomy of mood disorders is supported by noradrenergic brainstem system morphology. J. Affect. Disord. 54 (1-2), 217–224. https://doi.org/10.1016/S0165-0327(98)00168-2.

Behzadi, Y., Restom, K., Liau, J., Liu, T.T., 2007. A component based noise correction method (CompCor) for BOLD and perfusion based fMRI. NeuroImage 37 (1), 90–101. https://doi.org/10.1016/j.neuroimage.2007.04.042.

Bernard, R., Kerman, I.A., Thompson, R.C., Jones, E.G., Bunney, W.E., Barchas, J.D., Schatzberg, A.F., Myers, R.M., Akil, H., Watson, S.J., 2011. Altered expression of glutamate signaling, growth factor, and glia genes in the locus coeruleus of patients with major depression. Mol. Psychiatry 16 (6), 634–646. https://doi.org/10.1038/mp.2010.44.

Bijsterbosch, J.D., Ansari, T.L., Smith, S., Gauld, O., Zika, O., Boessenkool, S., Browning, M., Reinecke, A., Bishop, S.J., 2018. Stratification of MDD and GAD patients by resting state brain connectivity predicts cognitive bias. NeuroImage: Clin. 19, 425–433. https://doi.org/10.1016/j.nicl.2018.04.033.

Braak, H., Del Tredici, K., 2011. The pathological process underlying Alzheimer's disease in individuals under thirty. Acta Neuropathol. 121 (2), 171–181. https://doi.org/10.1007/s00401-010-0789-4.

Braak, H., Del Tredici, K., 2015. The preclinical phase of the pathological process underlying sporadic Alzheimer's disease. Brain 138 (10), 2814–2833. https://doi.org/10.1093/brain/awv236.

Braak, H., Thal, D.R., Ghebremedhin, E., Del Tredici, K., 2011. Stages of the pathologic process in alzheimer disease: age categories from 1 to 100 years. J. Neuropathol. Exp. Neurol. 70 (11), 960–969. https://doi.org/10.1097/NEN.0b013e318232a379.

Bürger, C., Redlich, R., Grotegerd, D., Meinert, S., Dohm, K., Schneider, I., Zaremba, D., Förster, K., Alferink, J., Bölte, J., Heindel, W., Kugel, H., Arolt, V., Dannlowski, U., 2017. Differential abnormal pattern of anterior cingulate gyrus activation in unipolar and bipolar depression: an fMRI and pattern classification approach. Neuropsychopharmacology 42 (7), 1399–1408. https://doi.org/10.1038/npp.2017.36.

Busse, A., Hensel, A., Guhne, U., Angermeyer, M.C., Riedel-Heller, S.G., 2006. Mild cognitive impairment: long-term course of four clinical subtypes. Neurology 67 (12), 2176–2185. https://doi.org/10.1212/01.wnl.0000249117.23318.e1.

Byers, A.L., Yaffe, K., 2011. Depression and risk of developing dementia. Nat. Rev. Neurol. 7 (6), 323–331. https://doi.org/10.1038/nrneurol.2011.60.

Chan-Palay, V., Asan, E., 1989. Quantitation of catecholamine neurons in the locus coeruleus in human brains of normal young and older adults and in depression. J. Comp. Neurol. 287 (3), 357–372. https://doi.org/10.1002/cne.902870307.

Cornwell-Jones, C.A., Palfai, T., Krasenbaum, D., Byer Jr., E., Clark, R., Kinnard, K., 1992. Housing influences exploration and social interaction of control and DSP-4-treated rats. Physiol. Behav. 52 (2), 271–276. https://doi.org/10.1016/0031-9384(92)90270-C.

Devilbiss, D.M., 2004. The effects of tonic locus ceruleus output on sensory-evoked responses of ventral posterior medial thalamic and barrel field cortical neurons in the awake rat. J. Neurosci. 24 (48), 10773–10785. https://doi.org/10.1523/JNEUROSCI.1573-04.2004.

Elman, J.A., Panizzon, M.S., Hagler Jr., D.J., Eyler, L.T., Granholm, E.L., Fennema-Notestine, C., Lyons, M.J., McEvoy, L.K., Franz, C.E., Dale, A.M., Kremen, W.S., 2017. Task-evoked pupil dilation and BOLD variance as indicators of locus coeruleus dysfunction. Cortex 97, 60–69. https://doi.org/10.1016/j.cortex.2017.09.025.

Folstein, M.F., Folstein, S.E., McHugh, P.R., 1975. Mini-mental state. J. Psychiatry Res. 12 (3), 189–198. https://doi.org/10.1016/0022-3956(75)90026-6.

Gannon, M., Wang, Q., 2019. Complex noradrenergic dysfunction in Alzheimer's disease: low norepinephrine input is not always to blame. Brain Res. 1702, 12–16. https://doi.org/10.1016/j.brainres.2018.01.001.

Gompf, H.S., Mathai, C., Fuller, P.M., Wood, D.A., Pedersen, N.P., Saper, C.B., Lu, J., 2010. Locus ceruleus and anterior cingulate cortex sustain wakefulness in a novel environment. J. Neurosci. 30 (43), 14543–14551. https://doi.org/10.1523/JNEUROSCI.3037-10.2010.

Gould, T.J., Adams, C.E., Bickford, P.C., 1997. Beta-adrenergic modulation of GABAergic inhibition in the deep cerebellar nuclei of F344 rats. Neuropharmacology 36, 75–81.

Granholm, E.L., Panizzon, M.S., Elman, J.A., et al., 2017. Pupillary responses as a biomarker of early risk for Alzheimer's disease. J. Alzheimer's Dis. 56, 1419–1428.

Green, R.C., Cupples, L.A., Kurz, A., Auerbach, S., Go, R., Sadovnick, D., Duara, R., Kukull, W.A., Chui, H., Edeki, T., Griffith, P.A., Friedland, R.P., Bachman, D., Farrer, L., 2003. Depression as a risk factor for Alzheimer disease: the MIRAGE study. Arch. Neurol. 60 (5), 753. https://doi.org/10.1001/archneur.60.5.753.

Grudzien, A., Shaw, P., Weintraub, S., Bigio, E., Mash, D.C., Mesulam, M.M., 2007. Locus coeruleus neurofibrillary degeneration in aging, mild cognitive impairment and early Alzheimer's disease. Neurobiol. Aging 28 (3), 327–335. https://doi.org/10.1016/j.neurobiolaging.2006.02.007.

Hamilton, M., 1960. A rating scale for depression. J. Neurol. Neurosurg. Psychiatry 23 (1), 56–62. https://doi.org/10.1136/jnnp.23.1.56.

Harro, J., Pähkla, R., Modiri, A.-R., Harro, M., Kask, A., Oreland, L., 1999. Dose-dependent effects of noradrenergic denervation by DSP-4 treatment on forced swimming and β-adrenoceptor binding in the rat. J. Neural Transm. 106 (7-8), 619–629. https://doi.org/10.1007/s007020050184.

Hoffer, B.J., Siggins, G.R., Oliver, A.P., et al., 1973. Activation of the pathway from locus coeruleus to rat cerebellar Purkinje neurons: pharmacological evidence of noradrenergic central inhibition. J. Pharmacol. Exp. Ther. 184, 553–569.

Hughes, C.P., Berg, L., Danziger, W., Coben, L.A., Martin, R.L., 1982. A new clinical scale for the staging of dementia. Br. J. Psychiatry 140 (6), 566–572. https://doi.org/10.1192/bjp.140.6.566.

Jack Jr., C.R., Bennett, D.A., Blennow, K., Carrillo, M.C., Dunn, B., Haeberlein, S.B., Holtzman, D.M., Jagust, W., Jessen, F., Karlawish, J., Liu, E., Molinuevo, J.L., Montine, T., Phelps, C., Rankin, K.P., Rowe, C.C., Scheltens, P., Siemers, E., Snyder, H.M., Sperling, R., Elliott, C., Masliah, E., Ryan, L., Silverberg, N., 2018. NIA-AA research framework: toward a biological definition of Alzheimer's disease. Alzheimer's Dementia 14 (4), 535–562. https://doi.org/10.1016/j.jalz.2018.02.018.

Jacobs, H.I.L., Wiese, S., van de Ven, V., Gronenschild, E.H.B.M., Verhey, F.R.J., Matthews, P.M., 2015. Relevance of parahippocampal-locus coeruleus connectivity to memory in early dementia. Neurobiol. Aging 36 (2), 618–626. https://doi.org/10.1016/j.neurobiolaging.2014.10.041.

Jacobs, H.I.L., Priovoulos, N., Poser, B.A., et al., 2020. Dynamic behavior of the locus coeruleus during arousal-related memory processing in a multi-modal 7T fMRI paradigm. *Elife* eLife Sciences Publications Ltd 9, 1–30.

Kelly, R.M., Strick, P.L., 2003. Cerebellar loops with motor cortex and prefrontal cortex of a nonhuman primate. J. Neurosci. 23 (23), 8432–8444. https://doi.org/10.1523/JNEUROSCI.23-23-08432.2003.

Maldjian, J.A., Laurienti, P.J., Kraft, R.A., Burdette, J.H., 2003. An automated method for neuroanatomic and cytoarchitectonic atlas-based interrogation of fMRI data sets. NeuroImage 19 (3), 1233–1239. https://doi.org/10.1016/S1053-8119(03)00169-1.

Martínez de la Iglesia, J., Onís Vilches, M.C., Dueñas Herrero, R., et al., 2002. The Spanish version of the Yesavage abbreviated questionnaire (GDS) to screen depressive dysfunc-tions in patients older than 65 years. MEDIFAM 12, 620–630.

Martuzzi, R., Ramani, R., Qiu, M., Shen, X., Papademetris, X., Constable, R.T., 2011. A whole-brain voxel based measure of intrinsic connectivity contrast reveals local changes in tissue connectivity with anesthetic without a priori assumptions on thresholds or regions of interest. NeuroImage 58 (4), 1044–1050. https://doi.org/10.1016/j.neuroimage.2011.06.075.

Menon, V., Uddin, L.Q., 2010. Saliency, switching, attention and control: a network model of insula function. Brain Struct. Funct. 214 (5-6), 655–667. https://doi.org/10.1007/s00429-010-0262-0.

Nakazato, T., 1987. Locus coeruleus neurons projecting to the forebrain and the spinal cord in the cat. Neuroscience 23 (2), 529–538. https://doi.org/10.1016/0306-4522(87)90074-1.

Nichols, T.E., Holmes, A.P., 2001. Nonparametric permutation tests for functional neuroimaging: a primer with examples. Hum. Brain Mapp. 15, 1–25.

Patel, A.X., Kundu, P., Rubinov, M., Jones, P.S., Vértes, P.E., Ersche, K.D., Suckling, J., Bullmore, E.T., 2014. A wavelet method for modeling and despiking motion artifacts from resting-state fMRI time series. NeuroImage 95, 287–304. https://doi.org/10.1016/j.neuroimage.2014.03.012.

Petersen, R.C., 2004. Mild cognitive impairment as a diagnostic entity. J. Intern. Med. 256 (3), 183–194. https://doi.org/10.1111/j.1365-2796.2004.01388.x.

Rajkowski, J., Kubiak, P., Aston-Jones, G., 1994. Locus coeruleus activity in monkey: phasic and tonic changes are associated with altered vigilance. Brain Res. Bull. 35 (5-6), 607–616. https://doi.org/10.1016/0361-9230(94)90175-9.

Robertson, B., Wang, L., Diaz, M.T., Aiello, M., Gersing, K., Beyer, J., Mukundan Jr, S., McCarthy, G., Doraiswamy, P.M., 2007. Effect of bupropion extended release on negative emotion processing in major depressive disorder: a pilot functional magnetic resonance imaging study. J. Clin. Psychiatry 68 (02), 261–267. https://doi.org/10.4088/JCP.v68n0212.

Sara, S., Bouret, S., 2012. Orienting and reorienting: the locus coeruleus mediates cognition through arousal. Neuron 76 (1), 130–141. https://doi.org/10.1016/j.neuron.2012.09.011.

Satterthwaite, T.D., Elliott, M.A., Gerraty, R.T., Ruparel, K., Loughead, J., Calkins, M.E., Eickhoff, S.B., Hakonarson, H., Gur, R.C., Gur, R.E., Wolf, D.H., 2013. An improved framework for confound regression and filtering for control of motion artifact in the preprocessing of resting-state functional connectivity data. NeuroImage 64, 240–256. https://doi.org/10.1016/j.neuroimage.2012.08.052.

Satterthwaite, T.D., Cook, P.A., Bruce, S.E., Conway, C., Mikkelsen, E., Satchell, E., Vandekar, S.N., Durbin, T., Shinohara, R.T., Sheline, Y.I., 2016. Dimensional depression severity in women with major depression and post-traumatic stress disorder correlates with fronto-amygdalar hypoconnectivty. Mol. Psychiatry 21 (7), 894–902. https://doi.org/10.1038/mp.2015.149.

Schwarz, L.A., Luo, L., 2015. Organization of the locus coeruleus-norepinephrine system. Curr. Biol. 25 (21), R1051–R1056. https://doi.org/10.1016/j.cub.2015.09.039.

Schwarz, L.A., Miyamichi, K., Gao, X.J., Beier, K.T., Weissbourd, B., DeLoach, K.E., Ren, J., Ibanes, S., Malenka, R.C., Kremer, E.J., Luo, L., 2015. Viral-genetic tracing of the input–output organization of a central noradrenaline circuit. Nature 524 (7563), 88–92. https://doi.org/10.1038/nature14600.

Sclan, S.G., Reisberg, B., 1992. Functional assessment staging (FAST) in Alzheimer's disease: reliability, validity, and ordinality. Int. Psychogeriatry 4 (3), 55–69. https://doi.org/10.1017/S1041610292001157.

Smith, S., Nichols, T., 2009. Threshold-free cluster enhancement: addressing problems of smoothing, threshold dependence and localisation in cluster inference. NeuroImage 44 (1), 83–98. https://doi.org/10.1016/j.neuroimage.2008.03.061.

Song, A.H., Kucyi, A., Napadow, V., Brown, E.N., Loggia, M.L., Akeju, O., 2017. Pharmacological modulation of noradrenergic arousal circuitry disrupts functional connectivity of the locus ceruleus in humans. J. Neurosci. 37 (29), 6938–6945. https://doi.org/10.1523/JNEUROSCI.0446-17.2017.

Strange, B.A., Henson, R.N.A., Friston, K.J., Dolan, R.J., 2000. Brain mechanisms for detecting perceptual, semantic, and emotional deviance. NeuroImage 12 (4), 425–433. https://doi.org/10.1006/nimg.2000.0637.

Szot, P., Franklin, A., Miguelez, C., Wang, Y., Vidaurrazaga, I., Ugedo, L., Sikkema, C., Wilkinson, C.W., Raskind, M.A., 2016. Depressive-like behavior observed with a minimal loss of locus coeruleus (LC) neurons following administration of 6-hydroxydopamine is associated with electrophysiological changes and reversed with precursors of norepinephrine. Neuropharmacology 101, 76–86. https://doi.org/10.1016/j.neuropharm.2015.09.003.

Theofilas, P., Ehrenberg, A.J., Dunlop, S., Di Lorenzo Alho, A.T., Nguy, A., Leite, R.E.P., Rodriguez, R.D., Mejia, M.B., Suemoto, C.K., Ferretti-Rebustini, R.E.D.L., Polichiso, L., Nascimento, C.F., Seeley, W.W., Nitrini, R., Pasqualucci, C.A., Jacob Filho, W., Rueb, U., Neuhaus, J., Heinsen, H., Grinberg, L.T., 2017. Locus coeruleus volume and cell population changes during Alzheimer's disease progression: a stereological study in human postmortem brains with potential implication for early-stage biomarker discovery. Alzheimer's Dementia 13 (3), 236–246. https://doi.org/10.1016/j.jalz.2016.06.2362.

Tsolaki, A.C., Kosmidou, V., Kompatsiaris, I., Papadaniil, C., Hadjileontiadis, L., Adam, A., Tsolaki, M., 2017. Brain source localization of MMN and P300 ERPs in mild cognitive impairment and Alzheimer's disease: a high-density EEG approach. Neurobiol. Aging 55, 190–201. https://doi.org/10.1016/j.neurobiolaging.2017.03.025.

Tsopelas, C., Stewart, R., Savva, G.M., et al., 2011. Neuropathological correlates of late-life depression in older people. Br. J. Psychiatry 198, 109–114.

van den Buuse, M., Lambert, G., Fluttert, M., Eikelis, N., 2001. Cardiovascular and behavioural responses to psychological stress in spontaneously hypertensive rats: effect of treatment with DSP-4. Behav. Brain Res. 119 (2), 131–142. https://doi.org/10.1016/S0166-4328(00)00349-1.

Van Dijk, K.R.A., Hedden, T., Venkataraman, A., Evans, K.C., Lazar, S.W., Buckner, R.L., 2010. Intrinsic functional connectivity as a tool for human connectomics: theory, properties, and optimization. J. Neurophysiol. 103 (1), 297–321. https://doi.org/10.1152/jn.00783.2009.

Wechsler, D., 1997. Wechsler Memory Scale - Third Edition (WAIS-III), 3rd ed. The Psychological Corporation.

Weinberg-Wolf, H., Fagan, N.A., Anderson, G.M., Tringides, M., Dal Monte, O., Chang, S. W.C., 2018. The effects of 5-hydroxytryptophan on attention and central serotonin neurochemistry in the rhesus macaque. Neuropsychopharmacology 43 (7), 1589–1598. https://doi.org/10.1038/s41386-017-0003-7.

Whitfield-Gabrieli, S., Nieto-Castanon, A., 2012. Conn: a functional connectivity toolbox for correlated and anticorrelated brain networks. Brain Connect. 2 (3), 125–141. https://doi.org/10.1089/brain.2012.0073.

Yin, Y., Hou, Z., Wang, X., Sui, Y., Yuan, Y., 2015. Association between altered resting-state cortico-cerebellar functional connectivity networks and mood/cognition dysfunction in late-onset depression. J. Neural Transm. 122 (6), 887–896. https://doi.org/10.1007/s00702-014-1347-3.

Zarow, C., Lyness, S.A., Mortimer, J.A., Chui, H.C., 2003. Neuronal loss is greater in the locus coeruleus than nucleus basalis and substantia Nigra in Alzheimer and Parkinson Diseases. Arch. Neurol. 60 (3), 337. https://doi.org/10.1001/archneur.60.3.337.

Zhang, S., Hu, S., Chao, H.H., Li, C.-S., 2016. Resting-state functional connectivity of the locus coeruleus in humans: in comparison with the ventral tegmental area/substantia Nigra pars compacta and the effects of age. Cereb. Cortex 26 (8), 3413–3427. https://doi.org/10.1093/cercor/bhv172.